Biomaterials 32 (2011) 4609–4620

Contents lists available at ScienceDirect

Biomaterials

journal homepage: www.elsevier.com/locate/biomaterials

The mechanism of enhancement on oral absorption of paclitaxel by N-octyl-O-sulfate chitosan micelles

Ran Mo [a], Xiang Jin [a], Nan Li [a], Caoyun Ju [a], Minjie Sun [b], Can Zhang [a,*], Qineng Ping [b]

[a] Center for Drug Discovery, China Pharmaceutical University, Nanjing 210009, PR China
[b] Department of Pharmaceutics, China Pharmaceutical University, Nanjing 210009, PR China

ARTICLE INFO

Article history:
Received 21 December 2010
Accepted 3 March 2011
Available online 26 March 2011

Keywords:
N-octyl-O-sulfate chitosan
Micelle
Paclitaxel
P-glycoprotein
Oral drug delivery

ABSTRACT

The overall objective of the present investigation was to demonstrate the effect of N-octyl-O-sulfate chitosan (NOSC) micelles on enhancing the oral absorption of paclitaxel (PTX) *in vivo* and *in vitro*, and identify the mechanism of this action of NOSC. *In vivo*, the oral bioavailability of PTX loaded in NOSC micelles (PTX-M) was 6-fold improved in comparison with that of an orally dosed Taxol®. In the Caco-2 uptake studies, NOSC micelles brought about a significantly higher amount of PTX accumulated in Caco-2 cells via both clathrin- and caveolae-mediated endocytosis, and NOSC had the effect on inhibiting PTX secreted by P-glycoprotein (P-gp), which was also proved by the studies on rhodamine 123 incorporated in NOSC micelles, fluorescence labeled micelles. The mechanism of NOSC on P-gp inhibition was demonstrated in connection with interfering the P-gp ATPase by NOSC rather than reducing the P-gp expression. Moreover, NOSC with the concentration approaching the critical micellar concentration (CMC) had the strongest effect on P-gp inhibition. In the Caco-2 transport studies, the presence of verapamil and NOSC both improved the transport of Taxol®, which further certified the effect of NOSC on P-gp inhibition, and PTX-M enhanced the permeability of PTX compared with Taxol®. The apparent permeability coefficient (Papp) of PTX-M decreased significantly at 4 °C in comparison with at 37 °C, which indicated a predominant active endocytic mechanism for the transport of PTX-M, a P-gp-independent way. Furthermore, the transcytosis of PTX-M was via clathrin-mediated rather than caveolae-mediated. In addition, the transepithelial electrical resistance (TEER) of Caco-2 cell monolayers had no significant change during the transport study, which pointed out that NOSC had no effect on opening the intercellular tight junctions. Based on the obtained results, it is suggested that NOSC micelles might be a potentially applicable tool for enhancing the oral absorption of P-gp substrates.

1. Introduction

Paclitaxel (PTX), an antineoplastic agent initially extracted from the bark of the Pacific yew tree (*Taxus brevifolia*), has a powerful antitumor ability against a wide spectrum of cancers, such as metastatic breast cancer, refractory ovarian cancer, colon caner, small and non-small cell lung cancer, and neck cancer [1]. It blocks cell replication by hyperstabilizing the cellular microtubules, therefore inhibits cellular growth and leads to apoptosis.

Due to the particularly low solubility (<0.03 mg/mL) [2] and poor permeability of PTX, it is classified under class IV of Biopharmaceutic Classification System (BCS) [3]. Clinically, PTX is currently dissolved in a 50/50 (v/v) mixture of Cremophore EL/dehydrated ethanol as commercial Taxol® or Paxene®, which is further diluted in isotonic saline solution before intravenous (i.v.) administration. Unfortunately, a series of major drawbacks associated with i.v. administration have emerged: (1) short-term physical stability (12–24 h) of diluted clinical formulation, (2) risk of catheter-related infection, (3) potential thrombosis and extravasation, (4) most severely, adverse effects mainly caused by Cremophore EL, such as hypersensitivity, hypotension, nephrotoxicity, neurotoxicity, etc [4]. Thus, other drug delivery systems have been considered and investigated to substitute i.v. administration.

Theoretically, oral administration of PTX is a preferable choice with various advantages: more convenience, better patient compliance, less cost and more chronic treatment regimens. However, the oral bioavailability of PTX is less than 10% [5], which is attributed to the following aspects: (1) the limited aqueous solubility and dissolution, (2) the multidrug efflux pump, P-glycoprotein (P-gp), (3) high affinity to intestinal and liver cytochrome P450 metabolic enzymes

* Corresponding author. Tel./fax: +86 25 83271171.
E-mail address: zhangcancpu@yahoo.com.cn (C. Zhang).

0142-9612/$ – see front matter © 2011 Elsevier Ltd. All rights reserved.
doi:10.1016/j.biomaterials.2011.03.005

(CYP450). In order to improve the bioavailability of PTX, co-administration with P-gp inhibitors, such as verapamil and cyclosporine A [6] has been performed to enhance the oral uptake of PTX. On the other hand, nanotechnology against cancer has being widely focused on by a large number of researchers throughout the world. The utilization of microemulsions [7], cyclodextrins [8], nanoparticles [9] and polymer micelles [10] to improve the oral absorption of PTX has been reported in succession. Polymeric micelles can accomplish the desire of a versatile drug carrier to enhance the bioavailability of PTX as a result of solubilization, P-gp or CYP450 inhibition by the polymers, and PTX delivery away from P-gp or CYP450 recognition. Qbal et al. prepared thiolated polymers (thiomers) by poly(acrylic acid)-cysteine conjugated with reduced glutathione (GSH), which acted as a P-gp inhibitor [11]. The oral administration of formulations containing PTX and thiomers improved the bioavailability of PTX. Dabholkar et al. prepared poly(ethylene glycol)$_{2000}$- phosphatidylethanolamine conjugate (PEG$_{2000}$-PE)/d-α-tocopheryl polyethyleneglycol 1000 succinate (TPGS) mixed micelles, which increased the Caco-2 uptake of rhodamine 123, a P-gp substrate [10]. Moreover, polymeric micelles have been used for oral administration vehicles of other drugs [12–14]. Cyclosporin A (CyA)-loaded PEG-b-poly(D, L-lactic acid) micelles prepared by Zhang et al. displayed higher bioavailability compared to Sandimmun Neoral® [15].

The P-gp inhibition mechanism of excipients (including nonionic surfactants (polyoxyethylene, polysorbate, vitamin-PEG succinate, block copolymer), PEG, derivates of β-cyclodextrin, and thiolated chitosan) is complicated, which mainly contains changing the fluidity of the cellular membrane, inhibiting P-gp ATPase and reducing P-gp expression. Zastre et al. demonstrated that methoxypolyethylene glycol-b-polycaprolactone (MePEG-b-PCL) increased the cellular accumulation and reduced the basolateral to apical flux of the P-glycoprotein substrate, rhodamine 123 (R-123) in Caco-2 cells by inhibiting P-gp through decreasing Caco-2 membrane fluidity while stimulating ATPase activity [16]. Collnot et al. found ATPase inhibition was an essential factor in the inhibitory mechanism of TPGS 1000 on cellular P-gp efflux pumps [17].

N-octyl-O-sulfate chitosan (NOSC), an amphipathic chitosan derivate, carrying sulfated groups as hydrophilic moieties and octyl groups as hydrophobic moieties was synthesized by our group [18]. The solubility of PTX in the micelles formed by self-assembly in water of NOSC was 1000-fold higher than that of free PTX in water.

In the context, the main purpose of the present study is to compare the oral bioavailability of PTX-loaded NOSC micelles (PTX-M) and Taxol®, identify NOSC as an inhibitor of P-gp, and assume a P-gp-independent micelle internalization for enhancement on oral absorption of PTX, which is manifested in Fig. 1. Moreover, the mechanism of NOSC on P-gp inhibition is investigated.

2. Materials and methods

2.1. Materials and animals

Chitosan (deacetylation degree of 92% and viscosity average molecular weight of 65 kDa) was purchased from the Shuanglin Biochemical Co. Ltd. (Nantong, China). N-octyl-O-sulfate chitosan (NOSC) was synthesized using the chitosan as described by our group [18], and the substitution of octyl degree and sulfonic degree were 0.38 and 2.56, respectively. Paclitaxel (PTX) was obtained from Yew Pharmaceutical Co. Ltd. (Jiangsu, China). Verapamil was offered by Hengrui Pharmaceutical Co. Ltd. (Jiangsu, China). Chlorpromazine, amiloride, nystatin were purchased from Sigma–Aldrich Co. (Shanghai, China). 3-(4,5)-dimethylthiahiazo(-z-yl-)-3,5-di-phenytetrazoliumromide (MTT) was offered by Amresco (Solon, Ohio, USA). Rhodamine 123 (R-123), cell lysis buffer for Western and IP, and BCA protein assay kit were provided by Beyotime Institute of Biotechnology (Jiangsu, China). Anti-Human CD243 (ABCB1) PE and Mouse IgG2a κ Isotype Control PE were purchased from eBioscience Inc. (San Diego, CA). Dulbecco's modified Eagle medium (D-MEM, high glucose), fetal bovine serum, penicillin-streptomycin solution, nonessential amino acid (NEAA) solution, Hank's buffered salt solution (HBSS), phosphate buffered saline (PBS) were provided by Thermo Fisher Scientific Inc. (Beijing, China). All other chemicals and reagents were analytical grade.

Sprague–Dawley (SD) rats (180–220 g) were purchased from the Shanghai Silaike Laboratory Animal Limited Liability Company. All the animals were pathogen free and allowed to access to food and water freely. Animal experiments were carried out in accordance with the Guidelines for Animal Experimentation of China Pharmaceutical University (Nanjing, China) and protocol was approved by the Animal Ethics Committee of this institution.

2.2. Pharmacokinetic studies

PTX-M was prepared by dialysis as described previously [18]. In brief, PTX (16 mg) and NOSC (16 mg) were dissolved in 0.355 mL dehydrated ethanol and 4 mL distilled water, respectively. The mass ratio between PTX and NOSC was 1:1. Subsequently, the PTX solution was added into the NOSC solution drop by drop with constant stirring. The mixed solution was subject to dialysis against 4 L deionized water for 12 h. The micelle solution was filtrated through a 0.45 μm pore-sized membrane. The drug-loading rate of PTX-M was about 40% and the PTX concentration of PTX-M was approximately 2.5 mg/mL.

The stability and integrity of PTX-M in the presence of mucin was investigated in vitro. PTX-M diluted at the different concentrations of PTX was mixed with pig mucin (Sigma–Aldrich) suspension at the concentration of 500 μg/mL in PBS (pH 7.4), and with PBS (pH 7.4) as control. After incubation at 37 °C for specified time, the samples were filtrated through a 0.45 μm pore-sized membrane. The content of PTX in the filtrates was determined by HPLC, and the size of filtrates was measured by dynamic light scattering (Zetasizer 3000 HAS, Malvern, UK). The PTX remaining ratio (R) was calculated by the following equation: Remaining ratio (%) = $C/C_{control} \times 100\%$, where C and $C_{control}$ were the concentrations of PTX in the filtrates with and without pig mucin, respectively. As shown in Table S1 (supporting information), the integrity of PTX-M remained in the presence of mucin.

To investigate the enhancement on the oral absorption of PTX by PTX-M, sixteen SD rats were divided randomly into the following groups ($n = 4$): (1) Taxol® (7 mg/kg, i.v.); (2) Taxol® (10 mg/kg, p.o.); (3) Taxol® (10 mg/kg, p.o.) with verapamil (25 mg/kg, p.o.); (4) PTX-M (10 mg/kg, p.o.). The total dose of NOSC given orally was about 15 mg/kg. Four formulations above were all diluted in saline at the PTX concentration of 1.2 mg/mL.

300 μL of blood samples were collected in eppendorf tubes at 0.0833, 0.1667, 0.25, 0.5, 1, 2, 4, 8 h following i.v. administration and 0.25, 0.5, 0.75, 1, 1.5, 2, 3, 5, 8, 12, 24, 36 h following three oral administration, and then centrifuged at 12,000 rpm for 10 min. The supernatant plasma was obtained and stored at −20 °C until HPLC analysis.

In order to examine the efficiency and bioavailability of PTX-M, the pharmacokinetic parameters were calculated using a non-compartmental model by Drug and Statistics for Windows (DAS ver 1.0), such as the area under the plasma concentration-time curve ($AUC_{0-\infty}$) for intravenous administration, $AUC_{0-36\ h}$ for oral administration, maximum concentration (C_{max}) and the time to C_{max} (T_{max}). In addition, the relative bioavailability (F %) of PTX from different oral formulations was examined as the following equation:

$$F\% = (AUC_{0-36\ h} \times D_{i.v.})/(AUC_{0-\infty} \times D_{p.o.}) \times 100\%,$$

where $AUC_{0-36\ h}$ and $AUC_{0-\infty}$ were the areas under the plasma concentration-time curve of PTX for the oral and intravenous administration, respectively. $D_{i.v}$ and $D_{p.o.}$ were the dosages of PTX for the intravenous and oral administration, respectively.

2.3. Caco-2 cells culture

Caco-2 cells (Passage: 44–54) were obtained from the cell bank of Chinese Academy of Sciences. The cells were cultured in d-mem with 10% (v/v) FBS, 1% (v/v) NEAA, 100 U/mL penicillin and 100 μg/mL streptomycin in an incubator (Thermo Scientific, USA) at 37 °C under an atmosphere of 5% CO_2 and 90% relative humidity. Cells were subcultivated approximately every 5 days (at 80% confluence) using trypsin-EDTA at a split ratio of 1:10.

2.4. Cytotoxicity studies

The cells were seeded at a density of 1×10^5 cells per well in 96-well plates (Costar, USA). After culture for 48 h, the culture medium was removed. 200 μL of the following test solutions and negative control (100 μL of non-complete culture medium (FBS free) with 100 μL of culture medium) were added into the wells. The test solutions were divided into four following groups: (1) NOSC; (2) PTX-M (PTX/NOSC, 1/1, w/w); (3) PTX-M (PTX/NOSC, 1/4, w/w); (4) Taxol®. The test solutions were diluted 5-fold, 7.5-fold and 10-fold in the non-complete culture medium. The cells were further cultured for 2 h. Subsequently, 20 μL aliquots of 5 mg/mL MTT PBS solution were added into each well, and then the cells were stained at 37 °C for 4 h. Thereafter, the medium was removed, and the cells were mixed with 150 μL of dimethyl sulfoxide (DMSO). The absorbance was measured at 570 nm by an ELIASA (Thermo Scientific, USA). Relative cell viability (R %) was calculated as follows:

$$R\% = absorbance_{test}/absorbance_{control} \times 100\%$$

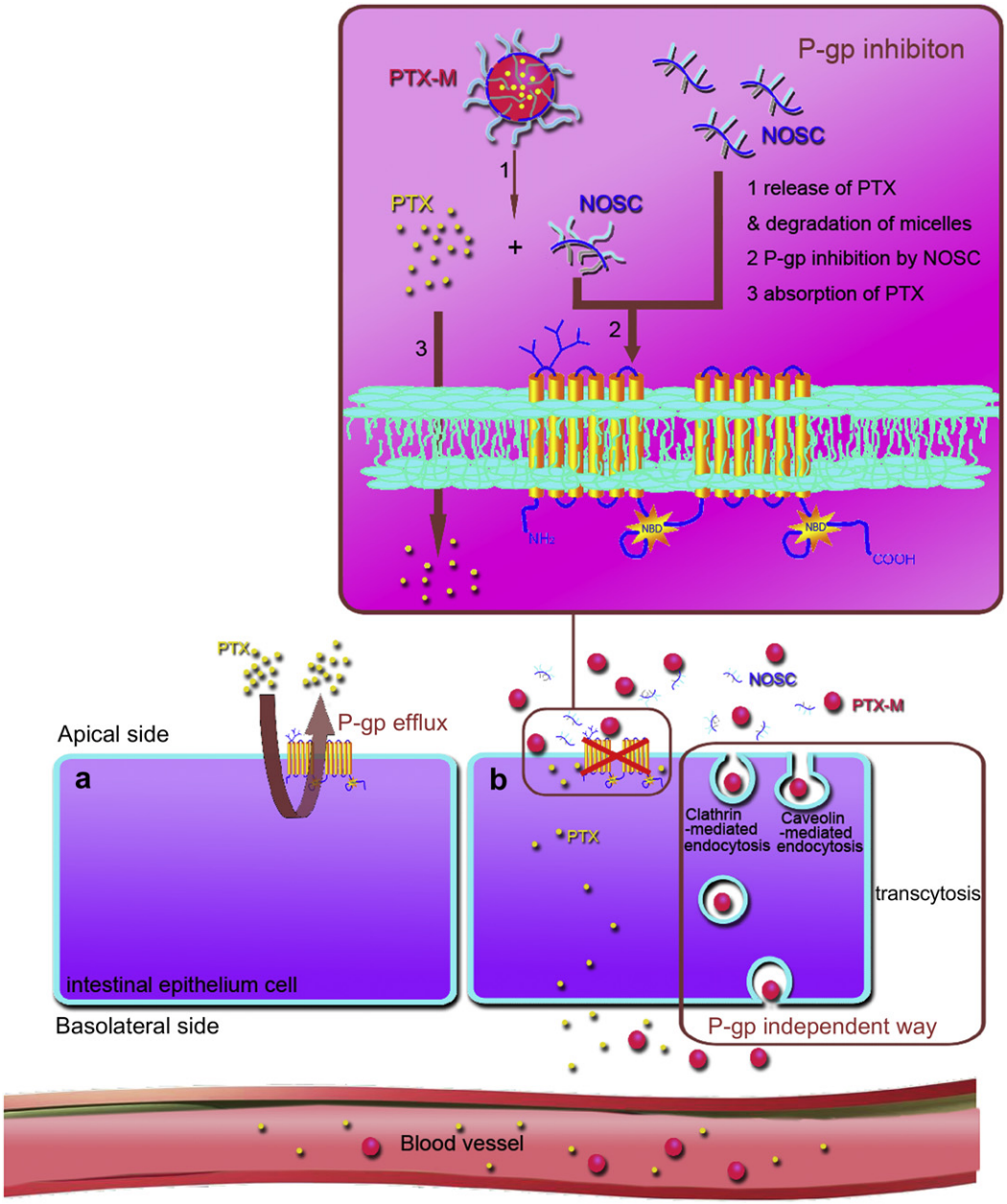

Fig. 1. Scheme of the effect of NOSC micelles on improving the oral absorption of PTX: (a): Inhibition of PTX absorption by the effect of the multidrug efflux transporter P-glycoprotein (P-gp) in the intestinal epithelium cells. (b): The hypothetical mechanism of enhancement on oral absorption of PTX by NOSC micelles.

2.5. Uptake studies

In order to estimate the enhancement on Caco-2 cells uptake of PTX by micelles endocytosis, and the mechanism of P-gp inhibition by NOSC, the following assays were performed.

2.5.1. Caco-2 cells accumulation of PTX studied by HPLC

The cells were seeded at a density of 1×10^5 cells per well in 24-well plates, and fed every two days for the first week and everyday thereafter. After 18–21 days, the cells were used for the uptake assays. Before experiments, the cells were washed twice with 37 °C HBSS. The uptakes of different formulations of PTX: Taxol® and PTX-M (PTX/NOSC, 1/4, w/w) were estimated on Caco-2 cells. The test solutions were diluted in the non-complete culture medium as 50, 67, 100 μg/mL concentrations of PTX, respectively. 400 μL of test solutions were added in the well and after culture at 37 °C for 2 h, the test solutions were removed. Subsequently, the cells were washed by 4 °C PBS (HyClone®, Thermo Scientific, USA) thrice, and the amount of PTX in Caco-2 cells were assayed by HPLC. Uptake ratio (U %) was calculated as the following equation.

$$U\% = Q_{PTX\,in\,cells}/Q_{cells\,protein} \times 100\%,$$

where $Q_{PTX\,in\,cells}$ and $Q_{cells\,protein}$ were the amounts of PTX in Caco-2 cells and cells protein, respectively.

2.5.2. Endocytosis pathways of PTX-M studied by HPLC

With the purpose of identifying the pathways of Caco-2 cells internalization used by PTX-M, the cells were first cultured with different specific agents for various kinds of endocytosis. After that, uptake study was carried out in the presence of the agent and PTX-M with 50 μg/mL PTX concentration.

Inhibition of clathrin-mediated endocytosis: the cells were first cultured with 20 μg/mL chlorpromazine [19] for 1 h at 37 °C and then uptake experiment was performed with PTX-M in the presence of 20 μg/mL chlorpromazine for 2 h at 37 °C.

Inhibition of caveolin-mediated endocytosis: the cells were first cultured with 15 μg/mL nystatin [20] for 1 h at 37 °C, and then uptake experiment was performed with PTX-M in the presence of 15 μg/mL nystatin for 2 h at 37 °C.

Inhibition of macropinocytosis: the cells were first cultured with 550 μM amiloride [21] for 1 h at 37 °C, and then uptake experiment was performed with PTX-M in the presence of 550 μM amiloride for 2 h at 37 °C.

Double inhibition of endocytosis: the cells were first cultured with two of the three agents above for 1 h at 37 °C, and then uptake experiment was performed with PTX-M in the presence of two of the three agents above for 2 h at 37 °C.

Thereafter, the test solutions were removed, and the cells were washed by 4 °C PBS thrice. The amount of PTX in Caco-2 cells was assayed by HPLC.

2.5.3. Inhibition of P-gp efflux pumps evaluated by HPLC

To evaluate the effect of NOSC on P-gp inhibition, the uptakes of different formulations of PTX: Taxol® of 50 μg/mL PTX, Taxol® with 100 μM verapamil, Taxol® with 0.4 mg/mL NOSC, PTX-M (PTX/NOSC, 1/4, w/w) of 50 μg/mL PTX, PTX-M (PTX/NOSC, 1/4, w/w) with 100 μM verapamil were tested on Caco-2 cells. After the cells were incubated with test solutions at 37 °C for 2 h, the test solutions were removed. Subsequently, the cells were washed by 4 °C PBS thrice, and the amount of PTX in Caco-2 cells were assayed by HPLC.

2.5.4. Inhibition of P-gp efflux pumps evaluated by fluorescence microscopy and flow cytometry

When fluorescent tagging was desired, R-123 was added to the micelle composition. Briefly, R-123 associated with PTX was dissolved in ethanol, and the other procedure of preparing R-123 loaded NOSC micelles (R-123-M) was similar to that of PTX-M. The different formulations of R-123: 5 μM of free R-123, free R-123 with 100 μM verapamil, free R-123 with 0.4 mg/mL NOSC, R-123-M and R-123 with 100 μM verapamil were evaluated on Caco-2 cells, respectively. The cells were seeded at a density of 1×10^5 cells per well in 6-well plates. After the cells reached a confluence of 80%, the cells were washed by PBS twice, and incubated with 1 mL of test solutions at 37 °C for 2 h. The cells were washed by 4 °C PBS thrice, and observed by fluorescence microscope (Olympus, Japan). Subsequently, the cells were trypsinized, and trypsinization was stopped by adding cold complete culture medium. After centrifugation at 4000 rpm for 5 min, the cells were washed thrice with PBS to remove extracellular R-123, and analyzed by flow cytometry (BD FACSCanto™, USA).

2.5.5. Inhibition of P-gp efflux pumps through reducing P-gp expression

To discern whether the effect of NOSC on P-gp was relative to reducing the P-gp expression, the amount of P-gp expression in Caco-2 cells was measured using a P-gp-antibody binding assay with Anti-Human CD243 (ABCB1) PE [22,23] as a P-gp monoclonal antibody, which were assayed by flow cytometric analysis. The different test solutions: 100 μM verapamil, 0.4 mg/mL NOSC and non-complete culture medium as control were studied on Caco-2 cells. The cells were seeded at a density of 1×10^5 cells per well in 6-well plates. After the cells reached a confluence of 80%, the cells were washed by PBS twice, and incubated with 1.5 mL of test solutions at 37 °C for 2 h. Then, the cells were washed by 4 °C PBS thrice, and trypsinized. Trypsinization was stopped by adding cold complete culture medium. After centrifugation at 4000 rpm for 5 min, the cells were washed thrice with PBS. 100 μL of the cells suspension was added 5 μL (0.5 μg) Anti-Human CD243 (ABCB1) PE solution. In addition, 100 μL of the blank cells suspension was added 5 μL Mouse IgG2a κ Isotype Control PE solution to obtain the cellular fluorescence. Then, the cells suspensions were incubated away from light at 25 °C for 0.5 h. After centrifugation at 4000 rpm for 5 min, the cells were washed by PBS trice to remove extracellular PE. The cells were analyzed by flow cytometry.

2.5.6. Inhibition of P-gp efflux pumps through interfering P-gp ATPase

In order to identify whether the effect of NOSC on P-gp was connected with interfering P-gp ATPase, the Pgp-Glo™ Assay System with P-gp (Promega, USA) were carried out. The Pgp-Glo™ assay detected the effects of compounds on recombinant human P-gp in a cell membrane fraction. The assay relied on the ATP dependence of the light-generating reaction of firefly luciferase, which was detected by Modulus™ Single Tube Multimode Reader. The test compounds were NOSC with different concentrations (1, 0.5, 0.4, 0.2, 0.05 mg/mL), Na_3VO_4 (100 μM, a selective inhibitor of P-gp), and verapamil (200 μM), respectively. Every procedure of this experiment followed the technical bulletin of the Pgp-Glo™ Assay Systems.

2.6. Transport studies of PTX-M across Caco-2 cells

The cells were seeded at a density of 1×10^5 cells per well on inserts (Millicell® cell culture inserts, Millipore, USA) containing permeable polycarbonate membrane in 24-well plates. The inserts were fed every two days for the first week and everyday thereafter. After 21–24 days, the cell monolayers were used for the transport experiment. The integrity of the cell monolayers was evaluated by measuring transepithelial electrical resistance (TEER) values using a Millicell® electrical resistance system (Millipore, USA). The cell inserts were used in the experiments when the resistance exceeded 350 Ω cm^2, which indicated that the tight junction of the cells was well-developed and the cell monolayers were integrated [24].

For all transport studies, the culture medium was removed and the cell monolayers were washed by 400 and 500 μL of 37 °C HBSS for the apical (AP) and basolateral (BL) side, respectively. After incubation with HBSS at 37 °C for 15 min, the HBSS was removed, and 400 μL of test solutions was added to the AP side while 500 μL of 37 °C fresh HBSS was added to the BL side of the inserts for estimating the AP to BL transport. 100 μL of solution in the BL side was sampled, and replaced with 37 °C fresh HBSS at 0.5, 1, 1.5, 2 h after incubation at 37 °C. 100 μL of sample was mixed with 100 μL of methyl cyanides, vortexed, and certificated. 50 μL of supernatant was injected in the HPLC system. At the end of experiment, TEER values were assayed to estimate the integrity of the cell monolayers.

The cumulative amount of PTX transporting the cell monolayers was plotted as a function of time. Apparent permeability coefficients (Papp) of PTX were calculated according to the equation:

$$\text{Papp} = (dQ/dt)/(A \times C_0),$$

where the dQ/dt (μg/s) was the drug permeation rate, A was the surface area of polycarbonate membrane (0.6 cm^2) and C_0 (μg/mL) was the initial concentration of PTX in AP.

To identify the effect of NOSC on P-gp inhibition and transcellular transport of PTX-M by Caco-2 endocytosis, the transport experiment was performed on Caco-2 cell monolayers for seven test groups as follows:

(1) 50 μg/mL PTX concentration of Taxol® (37 °C)
(2) 50 μg/mL PTX concentration of Taxol® with 100 μM verapamil (37 °C)
(3) 50 μg/mL PTX concentration of Taxol® with 0.4 mg/mL NOSC (37 °C)
(4) 50 μg/mL PTX concentration of PTX-M (37 °C)
(5) 50 μg/mL PTX concentration of PTX-M (4 °C)
(6) 50 μg/mL PTX concentration of PTX-M with 20 μg/mL chlorpromazine (37 °C)
(7) 50 μg/mL PTX concentration of PTX-M with 15 μg/mL nystatin (37 °C)

2.7. Paclitaxel quantification in plasma and cells samples by HPLC

HPLC was performed with an SHIMADZU 2010AT system. The mobile phase consisted of methanol and water (70/30, v/v). A C_{18} column (250 mm × 4.6 mm × 5 μm, Diamonsil, China) was employed for the separation of analytes at a flow rate of 1 mL/min. The detection wavelength was set at 227 nm and the column temperature was 35 °C. The retention time for paclitaxel was approximately 13.5 min.

Plasma concentrations of PTX were analyzed by the HPLC technique described above. PTX in the plasma was extracted by the organic solvent extraction method. In brief, 100 μL of plasma was mixed with 15-fold volume of absolute ether, vortexed for 5 min, and centrifuged at 4000 rpm for 10min. The supernatant organic solvent was transferred to a clean 2 mL eppendorf tube, and evaporated at 40 °C. The drug residue was redissolved in the mobile phase (methanol/water, 70/30, v/v). This solution was vortexed for 3 min and centrifuged at 10,000 rpm for 5 min. 50 μL of supernatant was injected into the HPLC system. Calibration curve in the concentration range from 0.052 to 5.2 μg/mL for PTX was prepared as $A = 61.054 \times C - 824.69$, where A was HPLC area and C was the concentration of PTX (μg/mL). The coefficients of variation (CV) for intra- and inter-assay were all within 5%.

PTX concentrations in Caco-2 cells were also determined by the same HPLC system above. Briefly, Caco-2 cells in the cell plates were disrupted by 200 μL of cell lysis buffer to release the drug in the cells. The cell suspension was obtained in lysis buffer by blowing air repeatedly and tenderly. After centrifugation at 12,000 rpm for 5 min, 20 μL of supernatant was used for BCA protein assay [25] to quantitate the cells protein. In addition, 100 μL of supernatant was mixed with equal-volume of methyl cyanides for protein precipitation, vortexed for 5 min, and centrifuged at 12,000 rpm for 10 min. 50 μL aliquots of the supernatant were injected into the HPLC system. Calibration curve in the concentration range from 0.1 to 20 μg/mL for PTX was prepared as $A = 50080 \times C - 9350.1$, and the coefficients of variation (CV) for intra- and inter-assay were all within 5%.

2.8. Statistical analysis

Results are given as mean ± S.D. Statistical significance was tested by two-tailed Student's *t*-test or one-way ANOVA. Statistical significance was set at $P < 0.05$, and extremely significance was set at $P < 0.01$.

3. Results and discussions

3.1. Pharmacokinetic studies

The plasma concentration-time curve of PTX after a single i.v. administration of Taxol® at 7 mg/kg was shown in Fig. 2a. The maximum concentration (C_{max}) of PTX was approximately 12.07 μg/mL, and the average value obtained for $AUC_{0-\infty}$ was 10.58 μg h/mL. The half-life ($t_{0.5}$) and mean residence time (MRT) were about 1.64 h and 1.73 h, respectively (data not shown).

The oral bioavailability of PTX loaded in NOSC micelles was estimated and compared with Taxol® with or without a P-gp inhibitor verapamil. The plasma concentration-time profiles and the pharmacokinetic parameters of the different PTX formulations

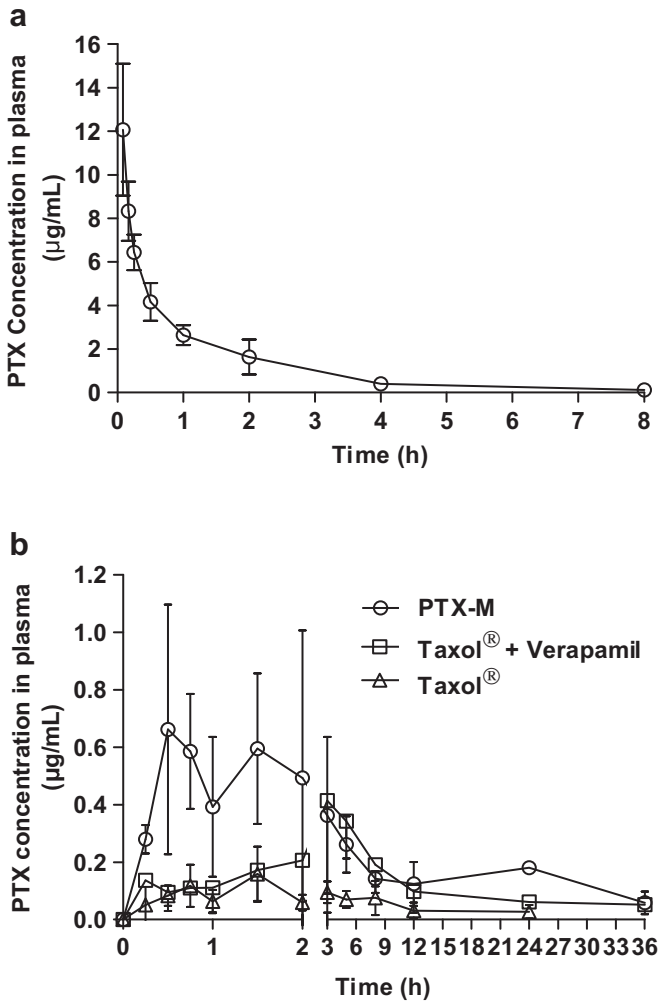

Fig. 2. Plasma concentration vs time curves of PTX after (a): i.v. administration of Taxol® at a dose of 7 mg/kg, and (b): after oral administration of PTX-M (PTX/NOSC, 1/1, w/w), Taxol® and Taxol® with 25 mg/kg verapamil within 36 h at a dose of 10 mg/kg to rats ($n = 4$).

administered orally were presented in Fig. 2 and Table 1, respectively. As shown in Fig. 2, the oral absorption of PTX was extremely limited even though administrated as the commercial formulation Taxol® with the bioavailability of 6.62% and $AUC_{0\text{-}36h}$ of 1.00 ± 0.76 μg h/mL, which was in agreement with previous reports [26]. co-administration of Taxol® and verapamil resulted in the enhancement on the absorption of PTX due to the effect of verapamil on P-gp inhibition. AUC_{0-36h} of co-administration of Taxol® and verapamil increased to 4.13 ± 0.21 μg h/mL, which was about 4-fold improved in comparison with Taxol® alone. Moreover, C_{max} was improved approximately 3-fold, and T_{max} extended to 4.33 ± 1.15 h, which was caused by the interaction between verapamil and P-gp located in the intestinal epithelial cells. In comparison with co-administration of Taxol® and verapamil, PTX-M was absorbed faster and revealed shorter time to reach C_{max} ($P < 0.05$). Furthermore, PTX loaded in NOSC micelles led to higher C_{max} (0.95 ± 0.18 μg/mL) and $AUC_{0\text{-}36h}$ (6.12 ± 0.99 μg h/mL). NOSC micelles increased the bioavailability of PTX to 40.50%, 6-fold improved in comparison with Taxol® alone, indicating that NOSC micelles showed a higher capacity to promote the oral absorption of PTX. The chitosan derivative micelles improved the bioavailability of PTX in many previous literatures. Li et al. prepared PTX loaded N-deoxycholic acid-N, O-hydroxyethyl chitosan (DHC) micelles, and after oral administration of PTX-loaded DHC micelles, the bioavailability was 3-fold improved compared with that of an orally dosed Taxol® [27].

PTX is a water-insoluble anti-cancer drug and a substrate of P-gp, which caused the poor bioavailability of PTX. co-administration of PTX and some P-gp inhibitors, such as verapamil, cyclosporin A, PSC 833 [28], KR30031 (a verapamil analog) [29], Syl611 (a taxane derivative) [30] were reported previously to improve the oral bioavailability of PTX. However, some shortages have been reported accompanying with these effects [31], including the toxicity, adverse effect by their pharmacology activities, interaction with other drugs by co-administration, etc. PTX incorporated NOSC micelles is a simple system displaying the highest capacity in solubilizing PTX, which is absence of additives, such as cremophor EL, a component of Taxol®, and what's more, the safety studies on NOSC consisted of acute toxicity study, intravenous stimulation study, injection anaphylaxis study, hemolysis study and cell viability assay were performed previously, which demonstrated NOSC micelles as a safe drug vehicle for oral administration [32].

In addition, PTX might be absorbed in intact micelles away from P-gp recognition, as a P-gp-independent way, and NOSC had the effect on inhibiting P-gp, which would be validated by the subsequent Caco-2 studies.

3.2. Cytotoxicity studies

The research and development of self-assembling polymeric micelles in the pharmaceutical field will count on several aspects including loading efficiency, potent to transport water-insoluble drugs and safety. The concentrations of PTX in PTX-M depended on the ratio of PTX and NOSC: PTX/NOSC (1/1, w/w) and PTX/NOSC (1/4, w/w) were about 2.5 mg/mL and 500 μg/mL, respectively, indicating high PTX loading efficiency. In order to evaluate the cytotoxicity of materials and determine the test PTX concentration on Caco-2 cells, the Caco-2 cells were treated with several concentrations of NOSC (from 2 mg/mL to 0.1 mg/mL), and PTX-M with various concentrations of PTX for 2 h, respectively, which were assessed using MTT assay. The results were exhibited in Fig. 3. The relative cell viability of PTX-M with PTX/NOSC (1/1, w/w) and PTX/NOSC (1/4, w/w) diluted 5-fold, 7.5-fold and 10-fold were both more than 80%, which implied no significant toxicity toward Caco-2 cells. Moreover, the different concentrations of NOSC had no

Table 1
Pharmacokinetic parameters of PTX after oral administration of PTX-M, Taxol® and Taxol® with verapamil at a dose of 10 mg/kg, and after i.v. administration of Taxol® at a dose of 7 mg/kg to rats (means ± SD, $n = 4$).

Parameter	PTX-M (10 mg/kg p.o.)	Taxol® + Verapamil (10 mg/kg p.o.)	Taxol® (10 mg/kg p.o.)	Taxol® (7 mg/kg i.v.)
C_{max} (μg/mL)	$0.95 \pm 0.18^{*}$	0.52 ± 0.32	0.18 ± 0.61	12.07 ± 3.03
T_{max} (h)	$1 \pm 0.87^{\#}$	4.33 ± 1.15	2 ± 0.87	0.08333
AUC_{0-36h} (μg × h/mL)	$6.12 \pm 0.99^{**, \#}$	$4.13 \pm 0.21^{**}$	1.00 ± 0.76	N/A
$AUC_{0-\infty}$ (μg × h/mL)	N/A	N/A	N/A	10.58 ± 1.72
F (%)	$40.50 \pm 6.58^{**, \#}$	$27.36 \pm 1.37^{**}$	6.62 ± 5.00	N/A

$^{*}P < 0.05$, vs Taxol® (p.o.), $^{\#}P < 0.05$, vs Taxol® + Verapamil (p.o.), $^{**}P < 0.01$, vs Taxol® (p.o.).

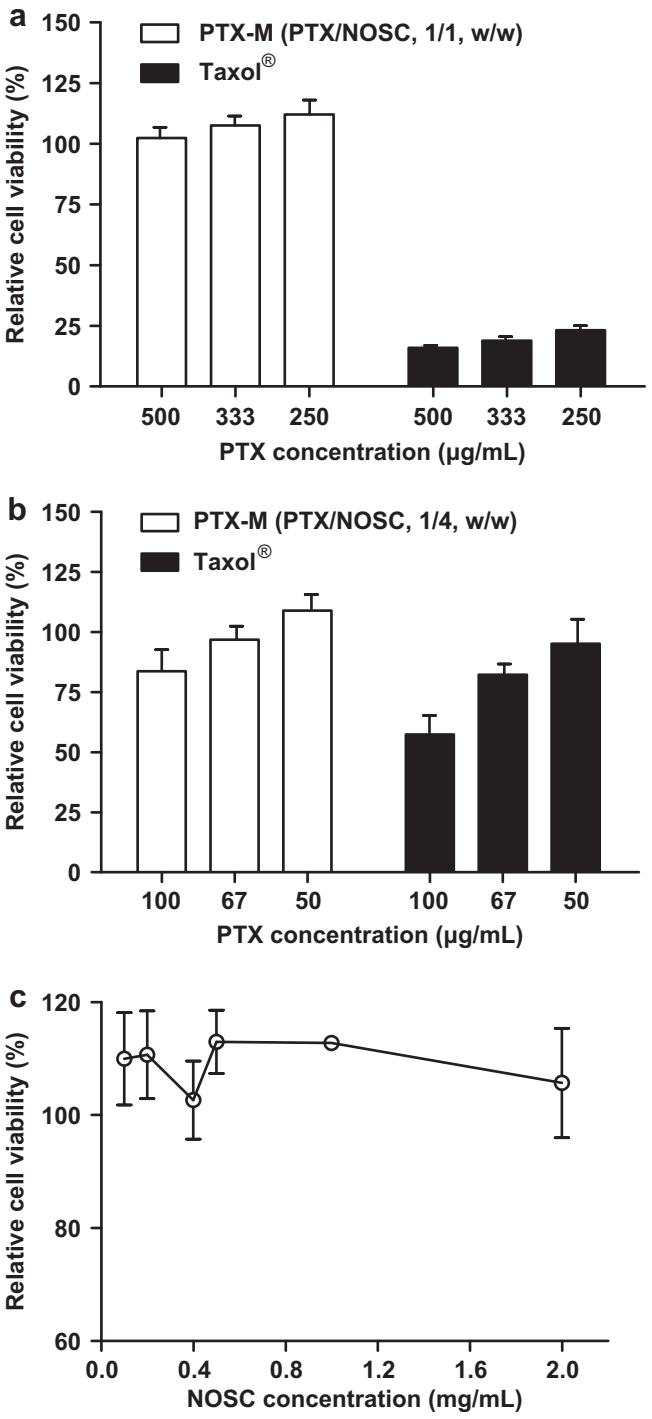

Fig. 3. Cytotoxicity of PTX-M, Taxol® and NOSC to Caco-2 cells. (a): PTX-M (PTX/NOSC, 1/1, w/w) and Taxol® with 500, 333, 250 μg/mL PTX; (b): PTX-M (PTX/NOSC, 1/4, w/w) and Taxol® with 100, 67, 50 μg/mL PTX; (c): NOSC with 2.0, 1.0, 0.5, 0.4, 0.2, 0.1 mg/mL concentration ($n = 6$).

toxicity to Caco-2 cells. By comparison, the cytotoxicity of Taxol® was also determined for 2 h. As shown in Fig. 3, the relative cell viability was in the range from 95.12 ± 9.53% to 57.40 ± 8.20% at concentrations of PTX below 100 μg/mL while the cell viability dramatically decreased thereafter. Thus, Taxol® with 500, 333, 250 μg/mL PTX would not be used to treat Caco-2 cells as control in comparison with PTX-M. Moreover, when PTX-M (PTX/NOSC, 1/1, w/w) was diluted to the concentrations of PTX below 100 μg/mL, the concentration of NOSC in PTX-M decreased below the critical micellar concentration (CMC, 0.45 mg/mL) of NOSC micelles [33], which might lead to instability of the micelles. Accordingly, PTX-M (PTX/NOSC, 1/4, w/w) and Taxol® with the PTX concentration of 100, 67, 50 μg/mL were chosen as the test formulations to evaluate the effect of NOSC micelles on enhancing the oral absorption of PTX through Caco-2 cells studies.

3.3. Uptake studies

3.3.1. Caco-2 cells accumulation of PTX

It is reported that nanocarriers, such as liposomes, nanoparticles, micelles, can enhance drug uptake of Caco-2 cells [10,34]. To investigate the ability of the NOSC micelles to improve Caco-2 cells uptake of PTX, the cells were treated with PTX-M with different concentrations of PTX (100, 67, 50 μg/mL) in comparison with Taxol®. As displayed in Fig. 4, Caco-2 cells uptake of PTX with 100, 67, 50 μg/mL concentrations of PTX-M were 15.15 ± 2.70, 15.19 ± 1.92, and 14.22 ± 1.15 μg/mg, which were 8.76-fold, 8.53-fold, and 9.88-fold higher than that of Taxol® at the same concentration of PTX, respectively ($P < 0.01$), indicating that PTX-M had a strong effect on increasing the Caco-2 cells uptake of PTX.

3.3.2. Endocytosis pathways of PTX-M

Different mechanisms of endocytosis have been reported [35]: clathrin-mediated endocytosis, caveolae-mediated endocytosis, macropinocytosis, adsorptive endocytosis, etc. In order to identify whether the enhancement on Caco-2 cells uptake of PTX was in connection with the cells internalization of PTX-M, and determine the endocytosis pathways of PTX-M, uptake experiments were performed in the presence of specific agents for different types of endocytosis. Results of the uptake studies are shown in Fig. 5. In comparison with Caco-2 cells uptake of PTX-M with 50 μg/mL PTX concentration in absence of endocytosis inhibitors as control, it could be demonstrated that different types of endocytosis inhibitors had different effects on internalization of micelles into Caco-2 cells. Incubation of Caco-2 cells with PTX-M in the presence of both chlorpromazine, a clathrin-mediated endocytosis inhibitor, and nystatin, a cavelin-mediated endocytosis inhibitor, resulted in the significant ($P < 0.01$) decrease of Caco-2 cells uptake of PTX-M, respectively, which indicated that clathrin and cavelin were involved in the internalization of PTX-M. On the contrary, the

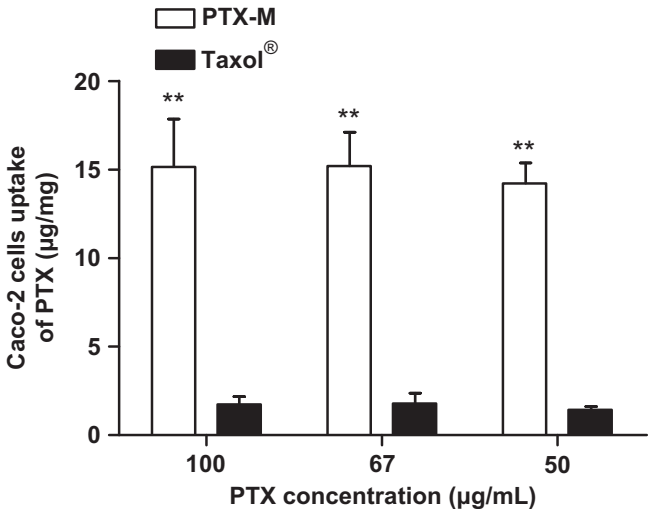

Fig. 4. Caco-2 cells uptake of PTX: PTX-M and Taxol® with 100, 67, 50 μg/mL PTX. ($n = 6$, $^{**}P < 0.01$ PTX-M vs Taxol® at the same concentration of PTX).

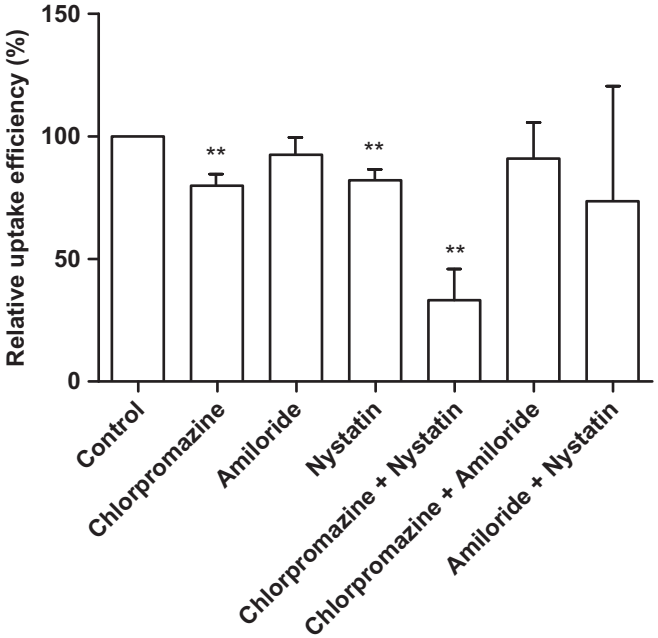

Fig. 5. Relative uptake efficiency of PTX-M with 50 μg/mL PTX in absence or presence of various endocytosis inhibitors ($n = 3$, $^{**}P < 0.01$ vs control).

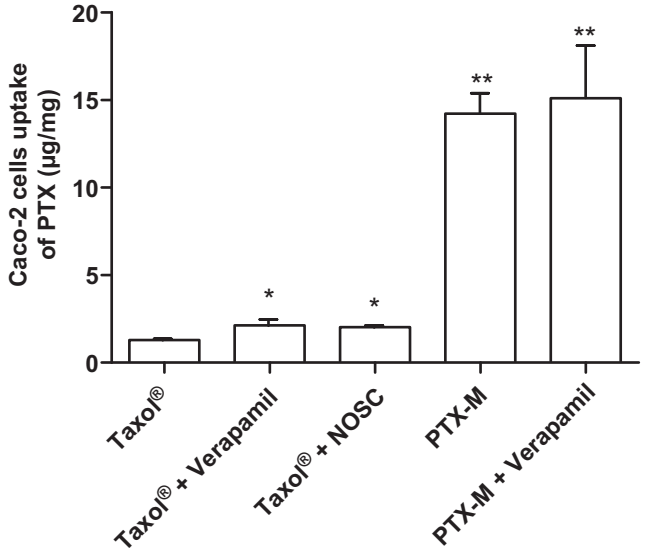

Fig. 6. Caco-2 cells uptake of PTX: Taxol®, Taxol® with verapamil, Taxol® with NOSC, PTX-M and PTX-M with verapamil diluted at 50 μg/mL PTX ($n = 3$, $^{*}P < 0.05$, $^{**}P < 0.01$ vs Taxol®).

presence of amiloride, a macropinocytosis inhibitor, had no effect on the uptake of PTX-M, implying that the endocytosis of PTX-M was not via macropinocytosis. Furthermore, double inhibition by chlorpromazine and nystatin resulted in the more decrease of PTX-M than single inhibition by one of them. There was an extremely significant difference ($P < 0.01$) in comparison with the uptake of control. Thus, the Caco-2 uptake of PTX-M was through clathrin- and cavelin-mediated endocytosis. To date, few investigation about endocytosis pathways of nanocarriers on Caco-2 cells were described in the literature. Gao et al. have found that wheat germ agglutinin-conjugated nanoparticles were also absorbed via both clathrin- and caveolae-mediated endocytosis [36]. In addition, Sahay et al. demonstrated that Pluronic P85 (P85) unimers internalized through caveolae-mediated endocytosis, while P85 micelles internalized through clathrin-mediated endocytosis [37].

3.3.3. Inhibition of P-gp efflux pumps

To assess a potential effect of NOSC on P-gp efflux pumps inhibition, which has been reported for other polymeric micelles [15], the impact of the polymer on the cells uptake of PTX, a typical P-gp substrate, was studied in comparison with that of verapamil, a traditional P-gp inhibitor. As PTX-M was diluted as 50 μg/mL concentration of PTX, the concentration of NOSC in PTX-M decreased to about 0.4 mg/mL. As shown in Fig. 6, in comparison with Taxol® (50 μg/mL PTX), the Caco-2 cells uptake of Taxol® with 100 μM verapamil increased significantly ($P < 0.05$) in comparison with that without verapamil. Interestingly, the presence of 0.4 mg/mL NOSC also improved remarkably the uptake of Taxol® ($P < 0.05$), which indicated that NOSC might have the effect on inhibiting P-gp efflux pumps. Moreover, there was no significant difference between the Caco-2 uptake of PTX-M in the presence and absence of verapamil, implying that PTX-M was internalized by Caco-2 cells as a P-gp-independent way.

In order to further demonstrate and intuitively observe the effect of NOSC micelles on the uptake of PTX, R-123 with a green fluorescence, which is a substrate of P-gp, is used as a marker for P-gp activity in Caco-2 cells. The fluorescence images of Caco-2 cells after incubation with 5 μM of free R-123 solution, free R-123 solution with 100 μM verapamil solution or 0.4 mg/mL NOSC solution, R-123-M solution, and R-123-M with 100 μM verapamil solution, respectively, were presented in Fig. 7. Moreover, the fluorescence intensities of Caco-2 cells incubated with solutions above were assayed by flow cytometry, which were shown in Fig. 8. In comparison with free R-123, both verapamil and NOSC elevated the amount of the internalized R-123, which was obtained from the quantity of R-123 fluorescence associated with the cells, although the fluorescence intensity of R-123 with NOSC was lower than that with verapamil. Accordingly, it was found that NOSC might have the effect on inhibiting R-123 secreted by P-gp. However, when Caco-2 cells were incubated with R-123-M, the presence or absence of verapamil did not influence R-123 accumulation in Caco-2 cells. The most evident explanation for this phenomenon is that in R-123 loaded NOSC micelles system, R-123 was in the cores of the micelles, and protected by the shells of the micelles, which disrupted the affinity between R-123 and P-gp, and thus inhibited R-123 efflux by P-gp. Consequently, R-123-M had the capability of bypassing the drug efflux by P-gp, indicating that polymeric micelle was a nice drug vehicle to delivery P-gp substrates including those for oral administration.

Based on these results, NOSC might have the ability to inhibit P-gp efflux pumps. The mechanism of the P-gp inhibition by the polymers is extremely complex, such as reducing P-gp expression, inhibiting or stimulating the ATP enzyme of P-gp, and changing the fluidity of the cellular membrane. Thus, in order to investigate the mechanism of P-gp inhibition by NOSC, the influence of NOSC on P-gp expression and P-gp ATPase were studied. In P-gp expression experiment, Caco-2 cells were treated with 100 μM verapamil solution or 0.4 mg/mL NOSC solution for 2 h. Anti-Human CD243 (ABCB1) PE, a monoclonal antibody of human Multidrug Resistant (MDR)-1, also known as P-gp and CD243, was used to mark the P-gp in Caco-2 cells, which was assayed by flow cytometry. The higher fluorescence intensity revealed the more amount of P-gp expression of Caco-2 cells. The results were shown in Fig. S1 (supporting information). It was indicated that there was a strong expression of P-gp in Caco-2 through removing the self fluorescence intensity of untreated Caco-2, which was marked by Mouse IgG2a κ Isotype Control PE. After cells treated for 2 h, 0.4 mg/mL NOSC had slight effect on reducing the expression of P-gp in Caco-2 cells, while

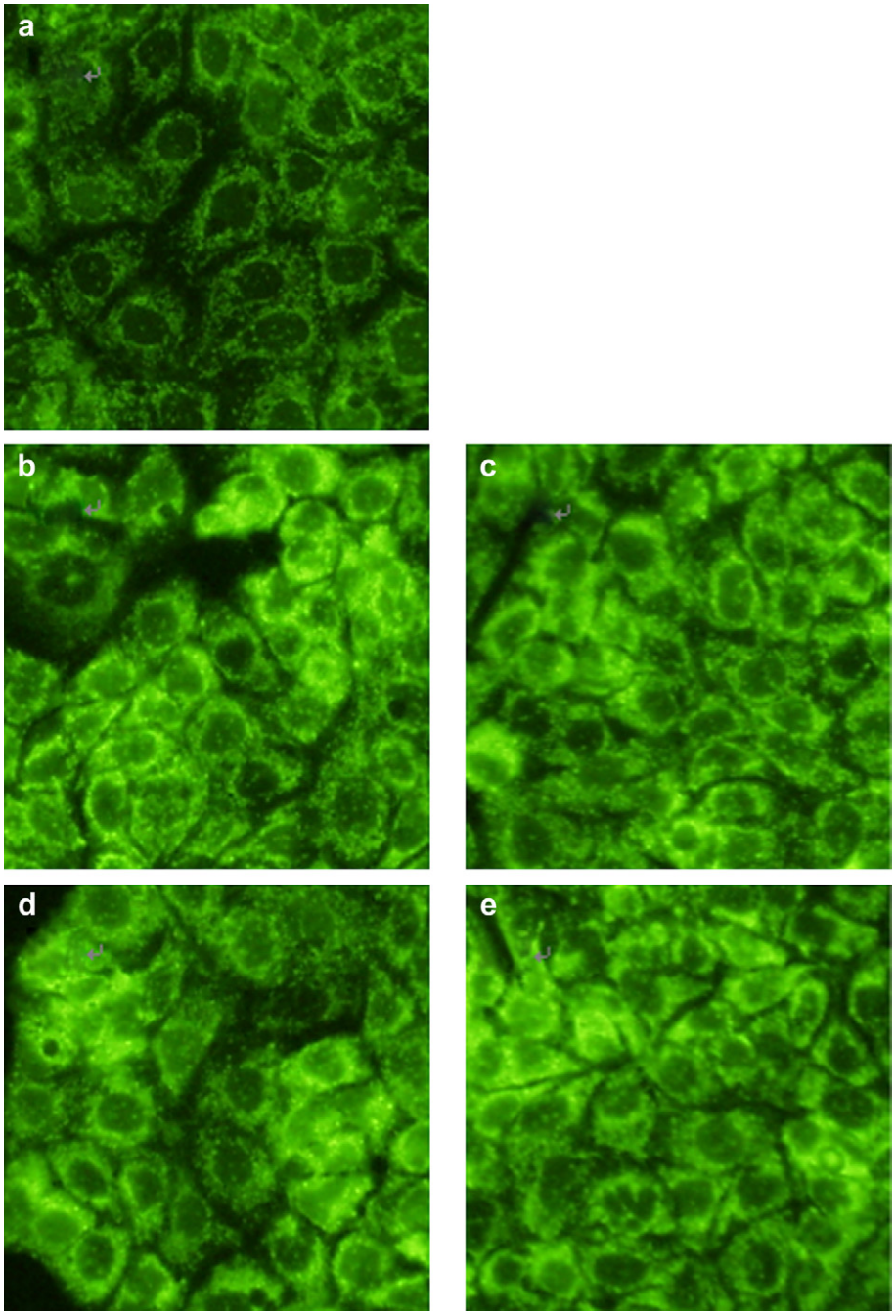

Fig. 7. Fluorescence microscopy of R-123 accumulation in Caco-2 cells: (a): 5 μM of free R-123, (b): free R-123 with NOSC, (c): free R-123 with verapamil, (d): R-123-M, and (e): R-123-M with verapamil.

verapamil at 100 μM concentration had stronger down-regulation effect. This result showed that the main mechanism of inhibiting P-gp efflux pumps by NOSC was not reducing the expression of P-gp.

In P-gp ATPase assay, the Pgp-Glo™ Assay System provides the necessary reagents for performing luminescent P-gp ATPase assays. The Pgp-Glo™ Assay relies on the ATP-dependence of the light-generating reaction of firefly luciferase. After a pool of ATP is first exposed to the P-gp ATPase, ATP consumption is detected as a decrease in luminescence from a second reaction with a recombinant firefly luciferase (Ultra-Glo™ Luciferase). The results of P-gp ATPase assay were shown in Table 2. Na_3VO_4 is a selective inhibitor of P-gp, and in the absence of Na_3VO_4, basal and drug-stimulated P-gp ATPase activities can be detected. ATP consumption in the presence of Na_3VO_4 is attributed to minor non-Pgp ATPase activities. As shown in Table 2, there was a significant drop in the average relative light units (RLU) in the untreated samples (NT) as compared to Na_3VO_4-treated samples. This decrease reflects the consumption of ATP by the basal P-gp ATPase activity and is expressed as $\triangle RLU_{basal}$. $\triangle RLU_{TC}$ represents the RLU decrease caused by a test compound in comparison with Na_3VO_4. If $\triangle RLU_{TC} > \triangle RLU_{basal}$, the test compound is a stimulator of P-gp ATPase activity. If $\triangle RLU_{TC} = \triangle RLU_{basal}$, the test compound has no effect on P-gp ATPase activity. If $\triangle RLU_{TC} < \triangle RLU_{basal}$, the test compound is a inhibitor of P-gp ATPase activity. Verapamil is

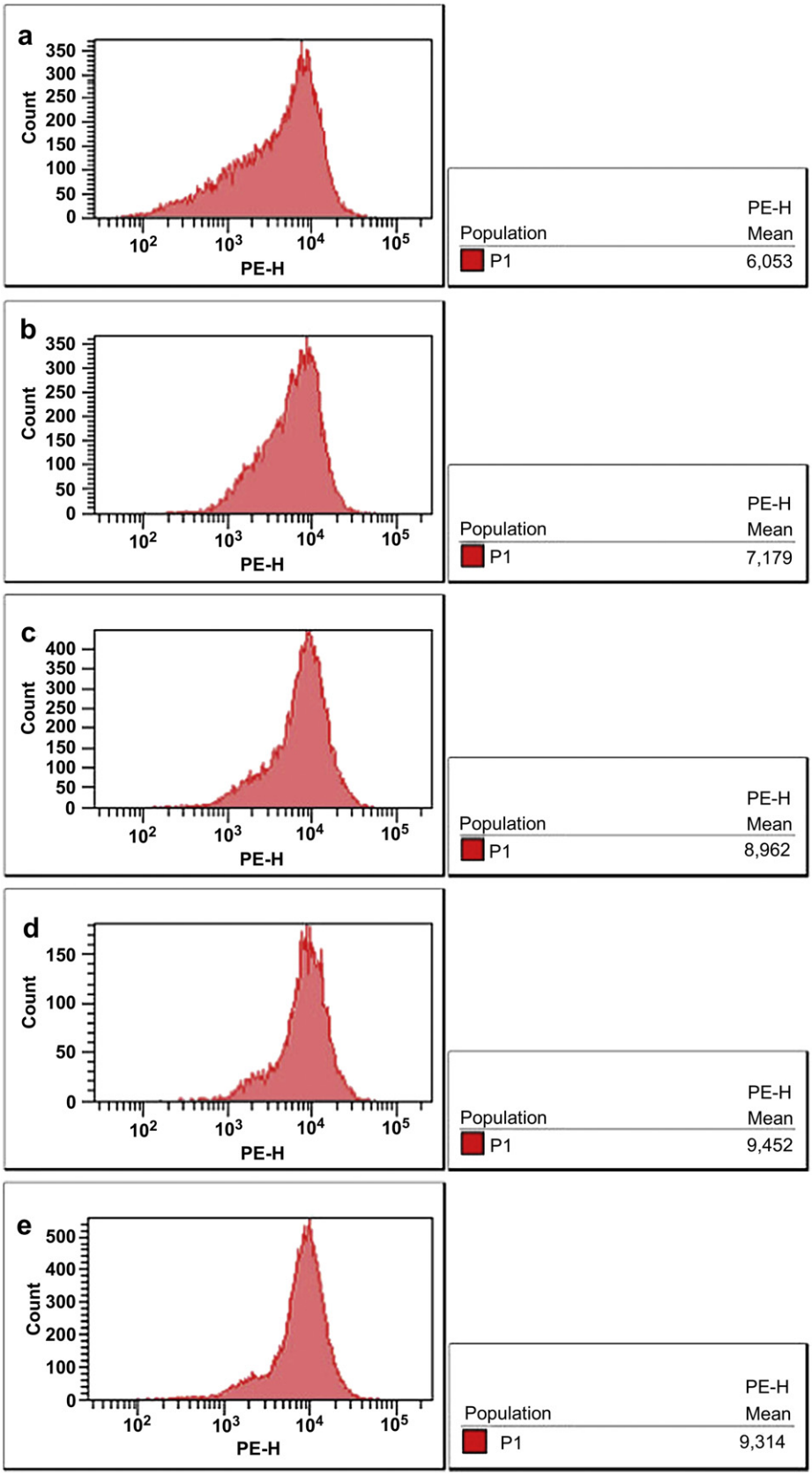

Fig. 8. Images of R-123 accumulation in Caco-2 cells by flow cytometry: (a): 5 μM of free R-123, (b): free R-123 with NOSC, (c): free R-123 with verapamil, (d): R-123-M, and (e): R-123-M with verapamil.

Table 2
Stimulation of P-gp ATPase activity by NOSC (means ± SD, $n = 3$).

	Na_3VO_4 (μM)	Untreated	Verapamil (μM)	NOSC (mg/mL)				
Concentration	100	N/A	200	1	0.5	0.4	0.2	0.01
RLU	846448 ± 127481	688235 ± 93387	347200 ± 78779	630773 ± 17328	624539 ± 46052	601984 ± 24078	615457 ± 56305	676804 ± 19697
ΔRLU		158213	499248	215675	221909	244464	230991	169644

a substrate for transport by P-gp that stimulates P-gp ATPase activity. The RLU decrease of verapamil reflects the consumption of ATP by verapamil-stimulated P-gp. The increase in P-gp ATPase activity caused by verapamil ($\triangle RLU_{TC}/\triangle RLU_{basal}$) is 499248/158213 = 3.15-fold. Interestingly, NOSC with the different concentrations also had the same effect with verapamil on stimulating P-gp ATPase activity, no matter that the concentration of NOSC lower or higher than CMC both resulted in the decrease of RLU. Moreover, NOSC with the concentration approaching CMC had the strongest effect on stimulation of P-gp ATPase activity, which indicated that NOSC could stimulate the P-gp ATPase activity, and inhibit PTX secreted by P-gp through consuming energy of P-gp. Therefore, the main mechanism of inhibiting P-gp efflux pumps by NOSC was interfering P-gp ATPase.

3.4. Transport studies

According to the results above, it was confirmed that NOSC micelles were able to enhance PTX accumulation in Caco-2 cells. However, the absorption of PTX into the circulatory system means that PTX transports across intestinal epithelial cells into the blood. In other words, internalized PTX in Caco-2 cells from the apical side should release and deliver to the basolateral side of Caco-2 monolayers. Thus, the well-established Caco-2 monolayers with the TEER higher than 300 Ω cm^2 were used to mimic the intestinal epithelial cells, and the higher values of apparent permeability coefficients (Papp) of PTX from the apical side to the basolateral side of Caco-2 monolayers indicated the greater permeability of PTX across the intestinal barrier.

In order to improve the oral bioavailability of PTX, one approach could be to enhance permeability of PTX across the intestine. To assess the capability of NOSC micelles on enhancing PTX transport, Caco-2 monolayers were treated with Taxol® of 50 μg/mL concentration of PTX, Taxol® with 100 μM verapamil, Taxol® with 0.4 mg/mL NOSC, and PTX-M of 50 μg/mL concentration of PTX, respectively, and the results are shown in Fig. 9. Although the components of Taxol® contain Cremophor EL, a surfactant that can inhibit P-gp efflux pumps, the Papp of Taxol® with 50 μg/mL concentration of PTX was $1.56 \pm 0.23 \times 10^{-6}$ cm/s, which was considerably low in accordance with the earlier reports [34]. It was implied that Taxol® as an oral administration formulation of PTX encountered with poorly oral absorption of PTX, which was demonstrated in pharmacokinetic studies above. A great amount of PTX as free form existed in the system of Taxol® with 50 μg/mL concentration of PTX, which was subjected to efflux by P-gp. The presence of verapamil increased significantly the Papp of Taxol® ($P < 0.01$). It was also found that the Papp of Taxol® with NOSC was higher than that of Taxol®. However, there was no significant difference on the Papp between Taxol® and Taxol® with NOSC ($P > 0.05$), due to the statistic error. On the basis of the results, it was deduced that NOSC had the effect on inhibition of P-gp efflux pumps, which was also confirmed in uptake studies. More importantly, the Papp of PTX-M was $8.55 \pm 0.90 \times 10^{-6}$ cm/s, which was approximately 5.5-fold improved in comparison with that of Taxol® ($P < 0.01$). It was indicated that PTX-M improved the oral absorption of PTX through two effects as follows. Firstly, NOSC as a polymeric material of PTX-M could inhibit free PTX released from PTX-M efflux by P-gp, and improve the delivery of PTX across intestinal barriers. Secondly, PTX loaded in NOSC micelles might be protected by the micelles away from P-gp, and thus, the interaction between P-gp and PTX was terminated. Accordingly, PTX transport throughout intestinal epithelial cells is enhanced notably by PTX-M.

Based on the demonstration that NOSC micelles had the ability to enhance PTX permeability through Caco-2 monolayers, the possible transport route of PTX-M was investigated. The potential mechanisms of nanoparticles including micelles for oral administration might be: (1) paracellular transport via tight junctions; (2) transcellular transport (passive or active) via the intestinal barrier; (3) lymphatic uptake via M cells of Peyer's patches.

The paracellular transport is corresponding to the passageway of molecules between epithelial cells. It has been reported that chitosan can open intercellular tight junctions to improve drug absorption [38]. The TEER of Caco-2 monolayers reflects the quality of tight junctions. A decrease of TEER manifests opening tight junctions, which means an increase of the paracellular permeability. In order to evaluate whether the chitosan derivative NOSC had the same effect with chitosan on opening tight junctions, the TEER of Caco-2 monolayers were measured during the transport studies. It was found that typical values were between 300 and 600 Ω cm^2 at 37 °C and higher than 600 Ω cm^2 at 4 °C, and no decrease was observed. Therefore, the integrity of Caco-2 cell monolayers was conserved. As a result, NOSC micelles with negative charge [33] could not open tight junctions, indicating that the mechanism of PTX-M transport was not paracellular transport via

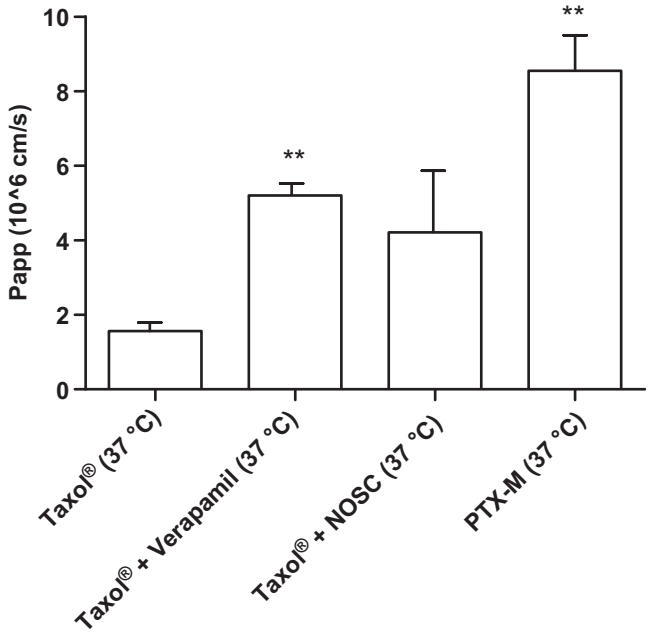

Fig. 9. Apparent permeability coefficients of PTX: Taxol®, Taxol® with verapamil, Taxol® with NOSC, PTX-M diluted at 50 μg/mL PTX at 37 °C ($n = 3$, $^{**}P < 0.01$ vs Taxol® at 37 °C).

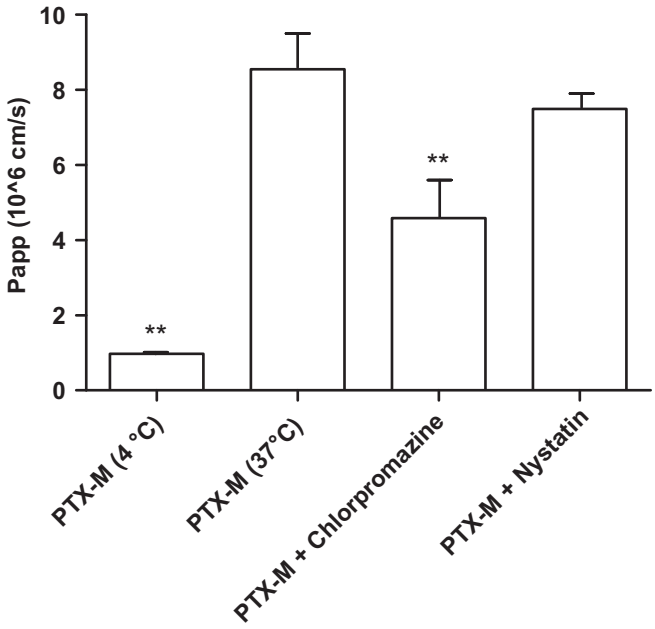

Fig. 10. Apparent permeability coefficients of PTX: PTX-M at 4 °C, PTX-M at 37 °C, PTX-M with chlorpromazine at 37 °C and PTX-M with nystatin at 37 °C ($n = 3$, $^{**}P < 0.01$ vs PTX-M at 37 °C).

tight junctions. This result was corresponding with the previous literature. Lin et al. have found that particles with negative charge could not disrupt tight junctions while particles with positive charge had the ability to open tight junctions [39].

The active uptake or transport of nanocarrier across Caco-2 monolayers, such as liposome [40], chitosan-coated lipid nanoparticles [41], chitosan-PLGA nanopaticles [42] have been demonstrated in previous publications. In order to assess whether the transport of PTX-M through Caco-2 monolayers is using vesicle-mediated transcytosis, Caco-2 monolayers were treated with PTX-M with 50 μg/mL concentration of PTX at 4 °C in comparison with at 37 °C. The results were presented in Fig. 10. The lower temperature (4 °C) is a general metablic inhibitor, and pinocytic/endocytic uptake of tracer molecules is usually hindered at this temperature [43]. As shown in Fig. 10, the Papp of PTX-M at 4 °C was $0.97 \pm 0.05 \times 10^{-6}$ cm/s, which was significantly lower than that at 37 °C ($P < 0.01$). Based on the results, it was deduced that 4 °C experiments typically account for cytoadhesion of PTX-M without internalization, which was in agreement with earlier works that demonstrated particles with size of 100–200 nm could be internalized by a receptor-mediated endocytosis, whereas larger particles had to be taken by phagocytosis [44]. On the basis of the results above that endocytosis of PTX-M was mediated via clathrin and caveolin, we sought to identify whether clathrin or cavolin was also implicated in transcytosis mechanisms. Transport experiments were performed in the presence of two inhibitors, nystatin and chlorpromazine. As the results shown in Fig. 10, the Papp of PTX-M in the presence of 15 μg/mL nystatin slightly decreased ($P > 0.05$), in comparison with that in the absence of nystatin. Nystatin, a caveolin-mediated endocytosis inhibitor, could disrupt the caveola structure. A significant decrease ($P < 0.05$) in the Caco-2 uptake of PTX-M was observed in the presence of nystatin (Fig. 5), whereas there was no significant decrease ($P > 0.05$) in the Caco-2 transport of PTX-M. Consequently, caveola was involved in the endocytosis rather than transcytosis of PTX. However, the presence of chlorpromazine, a clathrin-mediated endocytosis inhibitor, decreased the Papp of PTX-M notably ($P < 0.01$), which was implication of that clathrin was involved in both endocytosis and transcytosis mechanisms of PTX-M.

The result highlights the significance of the micelle nature on its intracellular trafficking, and reflects that NOSC micelles could open alternative opportunities for oral delivery of poorly soluble drugs.

4. Conclusion

In summary, we have demonstrated that NOSC micelles significantly improved the oral bioavailability of PTX compared with commercially available product (Taxol®) in vivo. The effect of NOSC micelles on enhancing the absorption of PTX was resulted from P-gp inhibition by NOSC, and the transport of PTX-M as a P-gp-independent way. Moreover, the mechanism of P-gp inhibition by NOSC was proved relative with interfering the P-gp ATPase rather than reducing the P-gp expression. In conclusion, this study suggests that NOSC micelles exhibit a potential to improve oral bioavailability of P-gp substrates.

Acknowledgments

This study is financially supported by Major Program for New Drug Discovery (2009ZX09310-004, 2009ZX09503-028), PhD Programs Foundation of Ministry of Education of China, (20090096110005) and 111 Project from the Ministry of Education of China and the State Administration of Foreign Expert Affairs of China (No. 111-2-07).

Appendix. Supplementary data

Supplementary data related to this article can be found online at doi:10.1016/j.biomaterials.2011.03.005.

References

[1] Rowinsky EK, Onetto N, Canetta RM, Arbuck SG. Taxol: the first of the taxanes, an important new class of antitumor agents. Semin Oncol 1992;19:646–62.
[2] Singla AK, Garg A, Aggarwal D. Paclitaxel and its formulations. Int J Pharm 2002;235:179–92.
[3] Kasim NA, Whitehouse M, Ramachandran C, Barnejo M, Lennernas H, Hussain AS, et al. Molecular properties of WHO essential drugs and provisional biopharmaceutic classification. Mol Pharmacol 2003;1:85–96.
[4] Szebeni J, Muggia FM, Alving CR. Complement activation by Cremophor EL as a possible contributor to hypersensitivity to PTX: an in vitro study. J Natl Cancer Inst 1998;90:300–6.
[5] Malingré MM, Beijnen JH, Schellens JH. Oral delivery of taxanes. Invest New Drugs 2001;19:155–62.
[6] van Asperen J, van Tellingen O, van der Valk MA, Rozenhart M, Beijnen JH. Enhanced oral absorption and decreased elimination of paclitaxel in mice cotreated with cyclosporin A. Clin Cancer Res 1998;4:2293–7.
[7] Nornoo AO, Zheng H, Lopes LB, Johnson-Restrepo B, Kannan K, Reed R. Oral microemulsions of paclitaxel: in situ and pharmacokinetic studies. Eur J Pharm Biopharm 2009;71:310–7.
[8] Agüeros M, Zabaleta V, Espuelas S, Campanero MA, Irache JM. Increased oral bioavailability of paclitaxel by its encapsulation through complex formation with cyclodextrins in poly(anhydride) nanoparticles. J Control Release 2010;145:2–8.
[9] Bhardwaj V, Ankola DD, Gupta SC, Schneider M, Lehr CM, Kumar MN. PLGA nanoparticles stabilized with cationic surfactant: safety studies and application in oral delivery of paclitaxel to treat chemical-induced breast cancer in rat. Pharm Res 2009;26:2495–503.
[10] Dabholkar RD, Sawant RM, Mongayt DA, Devarajan PV, Torchilin VP. Polyethylene glycol-phosphatidylethanolamine conjugate (PEG-PE)-based mixed micelles: some properties, loading with paclitaxel, and modulation of P-glycoprotein-mediated efflux. Int J Pharm 2006;315:148–57.
[11] Iqbal J, Sarti F, Perera G, Bernkop-Schnürch A. Development and in vivo evaluation of an oral drug delivery system for paclitaxel. Biomaterials 2010;32:170–5.
[12] Bromberg L. Polymeric micelles in oral chemotherapy. J Control Release 2008;128:99–112.
[13] Chiappetta DA, Hocht C, Taira C, Sosnik A. Efavirenz-loaded polymeric micelles for pediatric anti-HIV pharmacotherapy with significantly higher oral bioavailability. Nanomedicine 2010;5:11–23.
[14] Francis MF, Cristea M, Winnik FM. Exploiting the vitamin B12 p.thway to enhance oral drug delivery via polymeric micelles. Biomacromolecules 2005;6:2462–7.

[15] Zhang Y, Li X, Zhou Y, Fan Y, Wang X, Huang Y, et al. Cyclosporin A-loaded poly(ethylene glycol)-b-poly(d, l-lactic acid) micelles: preparation, in vitro and in vivo characterization and transport mechanism across the intestinal barrier. Mol Pharm 2010;7:1169–82.
[16] Zastre J, Jackson JK, Wong W, Burt HM. Methoxypolyethylene glycol-block-polycaprolactone diblock copolymers reduce P-glycoprotein efflux in the absence of a membrane fluidization effect while stimulating P-glycoprotein ATPase activity. J Pharm Sci 2007;96:864–75.
[17] Collnot EM, Baldes C, Wempe MF, Kappl R, Hüttermann J, Hyatt JA, et al. Mechanism of inhibition of P-glycoprotein mediated efflux by vitamin E TPGS: influence on ATPase activity and membrane fluidity. Mol Pharm 2007;4:465–74.
[18] Zhang C, Qu G, Sun Y, Wu X, Yao Z, Guo Q, et al. Pharmacokinetics, biodistribution, efficacy and safety of N-octyl-O-sulfate chitosan micelles loaded with paclitaxel. Biomaterials 2008;29:1233–41.
[19] Kitchens KM, Kolhatkar RB, Swaan PW, Ghandehari H. Endocytosis inhibitors prevent poly(amidoamine) dendrimer internalization and permeability across Caco-2 cells. Mol Pharm 2008;5:364–9.
[20] Perry JW, Wobus CE. Endocytosis of murine norovirus 1 into murine macrophages is dependent on dynamin II and cholesterol. J Virol 2010;84:6163–76.
[21] Koivusalo M, Welch C, Hayashi H, Scott CC, Kim M, Alexander T, et al. Amiloride inhibits macropinocytosis by lowering submembranous pH and preventing Rac1 and Cdc42 signaling. J Cell Biol 2010;188:547–63.
[22] Chaudhary PM, Mechetner EB, Roninson IB. Expression and activity of the multidrug resistance P-glycoprotein in human peripheral blood lymphocytes. Blood 1992;80:2735–9.
[23] Mechetner EB, Roninson IB. Efficient inhibition of P-glycoprotein-mediated multidrug resistance with a monoclonal antibody. Proc Natl Acad Sci U S A 1992;89:5824–8.
[24] Mathot F, des Rieux A, Ariën A, Schneider YJ, Brewster M, Préat V. Transport mechanisms of mmePEG750P(CL-co-TMC) polymeric micelles across the intestinal barrier. J Control Release 2007;124:34–43.
[25] Xu Y, Jin X, Ping Q, Cheng J, Sun M, Cao F, et al. A novel lipoprotein-mimic nanocarrier composed of the modified protein and lipid for tumor cell targeting delivery. J Control Release 2010;146:299–308.
[26] Sparreboom A, van Asperen J, Mayer U, Schinkel AH, Smit JW, Meijer DK, et al. Limited oral bioavailability and active epithelial excretion of paclitaxel (Taxol) caused by P-glycoprotein in the intestine. Proc Natl Acad Sci U S A 1997;94:2031–5.
[27] Li H, Huo M, Zhou J, Dai Y, Deng Y, Shi X, et al. Enhanced oral absorption of paclitaxel in N-deoxycholic acid-N, O-hydroxyethyl chitosan micellar system. J Pharm Sci 2010;99:4543–53.
[28] Bardelmeijer HA, Ouwehand M, Beijnen JH, Schellens JH, van Tellingen O. Efficacy of novel P-glycoprotein inhibitors to increase the oral uptake of paclitaxel in mice. Invest New Drugs 2004;22:219–29.
[29] Woo JS, Lee CH, Shim CK, Hwang SJ. Enhanced oral bioavailability of paclitaxel by coadministration of the P-glycoprotein inhibitor KR30031. Pharm Res 2003;20:24–30.
[30] Zhang Y, Li H, Wang H, Su F, Qu R, Yin D, et al. Syl611, a novel semisynthetic taxane derivative, reverses multidrug resistance by p-glycoprotein inhibition and facilitating inward transmembrane action. Cancer Chemother Pharmacol 2010;66:851–9.
[31] Constantinides PP, Wasan KM. Lipid formulation strategies for enhancing intestinal transport and absorption of P-glycoprotein (P-gp) substrate drugs: in vitro/in vivo case studies. J Pharm Sci 2007;96:235–48.
[32] Zhang C, Qu G, Sun Y, Yang T, Yao Z, Shen W, et al. Biological evaluation of N-octyl-O-sulfate chitosan as a new nano-carrier of intravenous drugs. Eur J Pharm Sci 2008;33:415–23.
[33] Zhang C, Ping Q, Zhang H. Self-assembly and characterization of paclitaxel-loaded N-octyl-O-sulfate chitosan micellar system. Colloids Surf B Biointerfaces 2004;39:69–75.
[34] Roger E, Lagarce F, Garcion E, Benoit JP. Lipid nanocarriers improve paclitaxel transport throughout human intestinal epithelial cells by using vesicle-mediated transcytosis. J Control Release 2009;140:174–81.
[35] Conner SD, Schmid SL. Regulated portals of entry into the cell. Nature 2003;422:37–44.
[36] Gao X, Wang T, Wu B, Chen J, Chen J, Yue Y, et al. Quantum dots for tracking cellular transport of lectin-functionalized nanoparticles. Biochem Biophys Res Commun 2008;377:35–40.
[37] Sahay G, Batrakova EV, Kabanov AV. Different internalization pathways of polymeric micelles and unimers and their effects on vesicular transport. Bioconjug Chem 2008;19:2023–9.
[38] Kotzé AF, Luessen HL, de Leeuw BJ, de Boer AG, Verhoef JC, Junginger HE. Comparison of the effect of different chitosan salts and N-trimethyl chitosan chloride on the permeability of intestinal epithelial cells (Caco-2). J Control Release 1998;51:35–46.
[39] Lin YH, Mi FL, Chen CT, Chang WC, Peng SF, Liang HF, et al. Preparation and characterization of nanoparticles shelled with chitosan for oral insulin delivery. Biomacromolecules 2007;8:146–52.
[40] Kapitza SB, Michel BR, van Hoogevest P, Leigh ML, Imanidis G. Absorption of poorly water soluble drugs subject to apical efflux using phospholipids as solubilizers in the Caco-2 cell model. Eur J Pharm Biopharm 2007;66:146–58.
[41] Prego C, García M, Torres D, Alonso MJ. Transmucosal macromolecular drug delivery. J Control Release 2005;101:151–62.
[42] Mi FL, Wu YY, Lin YH, Sonaje K, Ho YC, Chen CT, et al. Oral delivery of peptide drugs using nanoparticles self-assembled by poly(gammaglutamic acid) and a chitosan derivative functionalized by trimethylation. Bioconjug Chem 2008;19:1248–55.
[43] Hu Y, Litwin T, Nagaraja AR, Kwong B, Katz J, Watson N, et al. Cytosolic delivery of membrane-impermeable molecules in dendritic cells using pH-responsive core–shell nanoparticles. Nano Lett 2007;7:3056–64.
[44] Win KY, Feng SS. Effects of particle size and surface coating on cellular uptake of polymeric nanoparticles for oral delivery of anticancer drugs. Biomaterials 2005;26:2713–22.